DETAILED STUDY ON LARGE AREA 100% SOG SILICON MC SOLAR CELLS WITH EFFICIENCIES EXCEEDING 16%

A. Halm[1], J. Jourdan[1], S. Nichol[2], B. Ryningen[3], H. Tathgar[3], R. Kopecek[1]

[1]International Solar Energy Research Center - ISC - Konstanz, Rudolf-Diesel-Str. 15, D-78467 Konstanz, Germany.
Phone : +49 7531-3618350 ; Fax: +49 7531-3618311 ; Email : Andreas.Halm@isc-konstanz.de
[2]6N Silicon Inc., 1 Royal Gate Boulevard, Unit B, Vaughan Ontario, Canada L4L8Z7
[3]Umoe Solar AS, Fornebuveien 84, P.O. Box 60, 1324 Lysaker Norway

ABSTRACT: The focus of this work is the development and characterisation of 156x156 mm² sized industrial type screen printed silicon solar cells made of 100% solar grade silicon (SoG-Si). The feedstock under investigation is produced by 6N Silicon Inc. from metallurgical grade silicon with a lower cost low energy refining technique compared to the Siemens process. Solar cells were processed at ISC Konstanz with industrial type process equipment.
Defining a stable baseline process at ISC Konstanz, the improvements of the 6N Silicon material achieved during one year were tested against a single polysilicon reference brick. In addition, process enhancements leading to higher efficiencies were investigated.
Reaching the same average efficiency level for reference and 6N material applying the baseline process, an advanced process which still satisfies industrial production standards was defined. Running this advanced process achieved an average efficiency of 16.0% with 100% 6N Silicon feedstock, and a best cell having 16.3% efficiency. The four best cells of both materials and both processes are further characterised via SR, LBIC and thermography measurements to show material dependent characteristics on cell level. Reverse current behaviour and LID are tested for cells of different ingot positions which are relevant information for module manufacturers.

Keywords: solar grade silicon feedstock, industrial solar cell process, cell characterisation

1 INTRODUCTION

To satisfy the needs of the PV Industry, new solar grade silicon feedstocks are being designed to achieve lower cost levels while having higher impurities as compared to polysilicon feedstock that has been designed for the semiconductor industry. Multicrystalline solar cells made of solar grade silicon have a high potential for future green energy production, particularly as they can be manufactured at lower cost levels. SoG-Si producers like 6N Silicon Inc., Dow Corning, Timminco, or Globe emphasize the leading role of North America in this emerging sector of the PV industry. Satisfying the lower purity requirements for silicon specially made for PV applications, new refining techniques which are more basic and less energy intensive as the Siemens process are explored. This is beneficial for module prices and for energy payback time when similar efficiencies can be reached on SoG-Si compared to polysilicon [1]. Though some performance disparities were reported in the past, SoG-Si is now evolving towards the criteria set by industrial cell and module manufacturers. We have produced industrial type screen printed solar cells with efficiencies higher than 16% using 100% 6N Silicon SoG-Si. We have shown that for both processes applied at ISC the performance of cells made of the 100% 6N Silicon material is comparable to the reference cells made from polysilicon produced with the same process at the same time. We have performed detailed characterization to identify different properties of these two species of solar cells.

2 EXPERIMENTAL

2.1 Solar grade silicon

6N Silicon Inc. has developed a low temperature purification process for silicon through Al-Si melt segregation. The aluminium content of the feedstock end product, however, was observed to be lower than 0.05 ppmw. The overall contamination levels are sufficiently low to meet the needs of a solar cell producer. For the purpose of this study the feedstock was processed into multicrystalline silicon ingots with bulk resistivities between 0.4-2.7 Ωcm. A detailed description of the material purification process and the properties of the grown mc SoG ingots was already provided in [2].

2.2 Solar cell process

To be able to monitor changes in material quality over a long period of time, a stable baseline process is defined at ISC Konstanz. At the same time one brick with

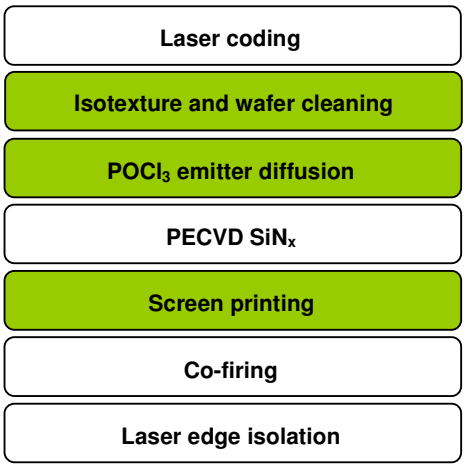

Figure 1: Process flow chart of ISC´s industrial baseline solar cell process.

500 neighbouring wafers of a polysilicon reference are laser coded and set aside. For each SoG-Si test run wafers of this reference material with positions equally distributed through the whole brick are included in the process. With stable process parameters these reference wafers are used to control the quality of the process. Figure 1 shows the process flow chart of the baseline process. It starts with laser coding of the substrates which is necessary to identify brick number and brick position. Then isotexture is applied in an industrial inline wet bench. Next, the emitter is diffused in a tube furnace followed by phosphorus glass removal and SiN_X anti reflective coating deposition. Thereafter metal contacts are screen printed on the substrates. Subsequently the contacts are formed in an IR belt furnace. In a last step p and n part are separated via laser edge isolation.

After reaching the same average efficiency for cells from SoG and polysilicon an advanced process was defined. It includes a novel isotexture, a shallow $POCl_3$ diffusion which is adapted to the needs of the SoG silicon, new metallisation paste and a new front side grid design (enhanced process steps are highlighted in green in Figure 1).

2.3 Efficiency development

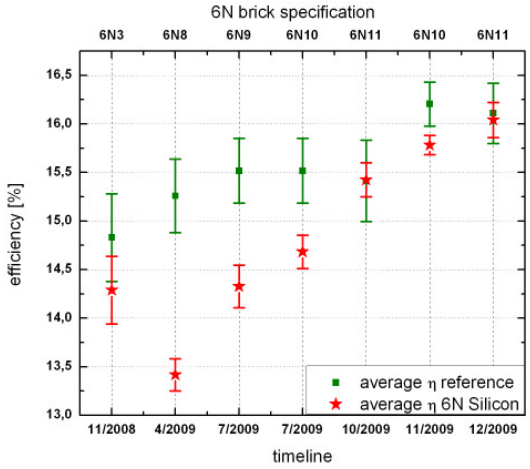

Figure 2: Efficiency improvements of the SoG-Si cells due to material and process improvements.

Figure 2 shows the development of the average efficiencies reached at ISC with 6N Silicon and reference material. Stars mark the average values of the SoG cells with standard deviation, squares the reference cells. For each experiment 30 wafers of a 6N brick are compared against 20 references. Starting from 4/2009 the emitter sheet resistance is adjusted from 45 Ω/□ to 55 Ω/□. In 7/2009 the adapted isotexture is introduced which is also effective on the SoG wafers. Beforehand ISC´s standard isotexture was applied without noticeable effect. Then, until 10/2009 the baseline process is kept stable with an efficiency limit of 15.5% for the reference material. This limit is reached with 6N Silicon`s material 6N11 in 10/2009. From this point on the advanced cell process with improved diffusion and metallisation is applied on the two latest materials 6N10 and 6N11. Efficiencies of 16.04% average and a best cell of 16.33% are reached on 6N11 in 12/2009 compared to 16.11% (best cell: 16.60%) on the reference.

3 CELL CHARACTERISATION

Detailed characterisation of the SoG-Si solar cells as compared to the reference cells from polysilicon helps to understand the different properties and potential of SoG-Si.

3.1 IV measurements

IV measurements are performed with a GP sun test equipment under one sun illumination.

Table 1: average IV results for both processes and materials.

		η [%]	J_{SC} [mA/cm²]	V_{OC} [mV]	FF [%]
baseline process	6N Silicon average	15.4	32.4	615.1	77.5
	best cell	15.7	32.7	617.5	78.1
	reference average	15.4	32.7	609.1	77.4
	best cell	16.1	33.6	616.5	77.8
advanced process	6N Silicon average	16.0	33.3	620.9	77.6
	best cell	16.3	33.4	625.4	78.2
	reference average	16.1	33.9	616.1	77.1
	best cell	16.6	34.2	623.3	77.7

Table 1 displays average IV results for the best 6N brick tested (6N11) and its reference processed simultaneously. Below the average results the best cell of each batch is shown. For the baseline process average efficiencies of 6N and reference cells are identical. As typical for SoG-Si the solar cells made of 100% 6N Silicon feedstock show a higher open circuit voltage and fill factor but lower short circuit current. The higher V_{OC} and FF are mainly based on lower bulk resistivity and higher equilibrium carrier density. The lower J_{SC} originates mostly from a lower diffusion length and reduced carrier mobility due to compensation and remaining contaminants. The average efficiency though is identical for both materials applying the baseline process and with 16.0% average only 0.1% absolute lower for the SoG cells applying the advanced process.

The four best cells of both processes and materials are characterised further with SR, LBIC and thermography. Breakdown voltage (V_{BD}), reverse current and light induced degradation (LID) depend amongst others on the net acceptor density. That is why they are tested on cells from different positions along the brick.

3.2 Spectral response measurements

Spectral response was measured for the best four cells of both materials and both processes. Table 1 shows the efficiency and short circuit current for these cells. As can be observed in the graphs in Figure 3, both materials show a significantly enhanced blue response for the advanced process. This effect originates from reduced recombination in the shallow 65 Ω/□ emitter and is even more pronounced taking into account that the reflectivity for the advanced process cells is higher than for the baseline cells between 350 and 550 nm.

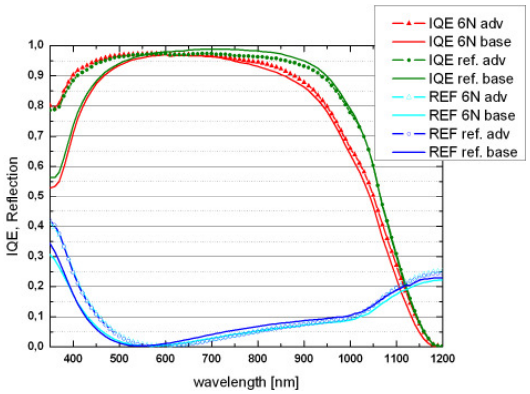

Figure 3: internal quantum efficiency (IQE) and reflection (REF) plots of the best cells for the advanced and baseline process of reference and 6N Silicon material; 6N cells are labeled "6N", reference cells "Ref", baseline process cells are labeled "base", advanced process cells "adv".

Comparing both cells of the 6N Silicon material another effect can be observed. The IQE between 800 and 1200 nm for the advanced process cell is higher than the one for the baseline cell. Because this part of the spectrum is mostly absorbed in the bulk part of the cell this leads to the conclusion that the slightly longer diffusion process promotes a stronger internal gettering effect. This is beneficial for bulk lifetime which can be seen in the IQE. The difference in IQE for long wavelengths regarding cells from polysilicon and 6N material shows the limitations of the SoG-Si. For both processes, the SoG-Si cells perform lower in the bulk region due to a lower diffusion length.

3.3 LBIC maps

Light beam induced current mappings with a resolution of 500 µm were recorded for the same cells mentioned above. These maps are a convenient way to check the homogeneity of the cell response throughout the cell area.

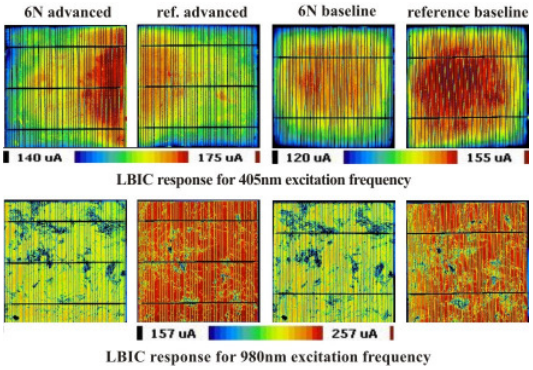

Figure 4: LBIC maps for the four best cells; cells are organized in columns beginning with the 6N advanced process cell, the first row shows 405nm maps, the second one maps for 980 nm.

Studying the maps for 405 nm shown in figure 3 the advanced and baseline process cells have to be regarded separately. The response of the 6N advanced cell is better than the one of its reference. That means that the conversion efficiency in the emitter region is not limited by material properties. For the baseline cells a small difference is visible favouring the reference cell. The maps for 980 nm on the bottom of Figure 4 give information about the bulk response of the cells. All maps have the same colourscale. Comparing the 6N cells against the references a clear difference in bulk conversion efficiency is visible as seen before in the IQE. The advanced process reference cell obviously performs slightly better in all regions than the baseline reference. The map of the 6N advanced cells appears to be the same as the 6N baseline cell. Taking a closer look though reveals that e.g. the low performing structure in the middle of both cells is less pronounced for the advanced process cell.

As can be observed for all maps the overall homogeneity of the processes is comparable for both materials. Since this study is made on mc material, grain dependent performance disparities are expected.

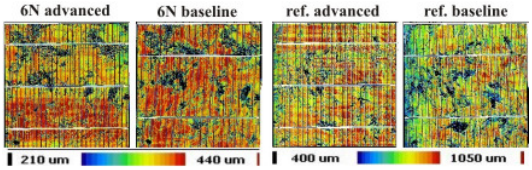

Figure 5: LBIC diffusion length maps for the four best cells.

Figure 5 shows LBIC diffusion length maps of the same cells. For the 6N cells a small improvement is visible favouring the advanced process cell. Low performing regions are less pronounced which leads to a higher mean value. For the reference cells the difference is even more pronounced. Their mean diffusion lengths are nearly 80 µm apart with 757 µm and 680 µm. Having a mean value of 376 µm and 360 µm respectively the 6N material has a sufficiently high diffusion length to result in a high performing solar cell. Here the influence of the compensation on carrier mobility becomes visible. The diffusion length of the cells from SoG-Si is only half compared to the reference but still high enough to not limit cell efficiency for the applied processes.

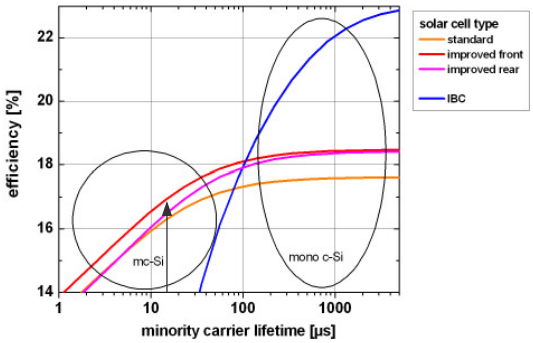

Figure 6: efficiency potential vs. substrate lifetime for different cell designs.

Figure 6 shows a simulation of the efficiency potential for different cell concepts in dependence of the substrate minority carrier lifetime. The simulation was run in PC1D taking the best 6N cell as a starting point. For our standard cell concept on mc substrates 16.3% are feasible which corresponds to a substrate lifetime of

approximately 15 µs. In this regime enhancements of the rear side of the cells will not lead to significant improvements as can be seen in the graph (purple line). IBC cell design on this material would not be useful at all. For realising higher efficiencies with the 6N material the next step is to improve the front side (e.g. selective emitters) with a potential efficiency limit of 17 % (red line).

4 OPERTING CHARACTERISTICS

For PV module manufacturers high conversion efficiency on cell level is a good criteria for solar cell selection. Additionally important on module level are reverse characteristics and light induced degradation (LID) of the individual cells. The first decides about how many bypass diodes have to be used in a module, the second is a measure for the power loss suffered referred to the initial power output.

For the comparison of reverse characteristics and LID 6N Silicon SoG cells and references of the bottom middle and top part of a brick are compared in these respects to polysilicon reference cells from similar positions.

4.1 Thermography images

Lock-In-Thermography images under infrared illumination were recorded for the four cells characterised before to give a qualitative characterisation of cell shunting. Figure 7 shows the results for these cells.

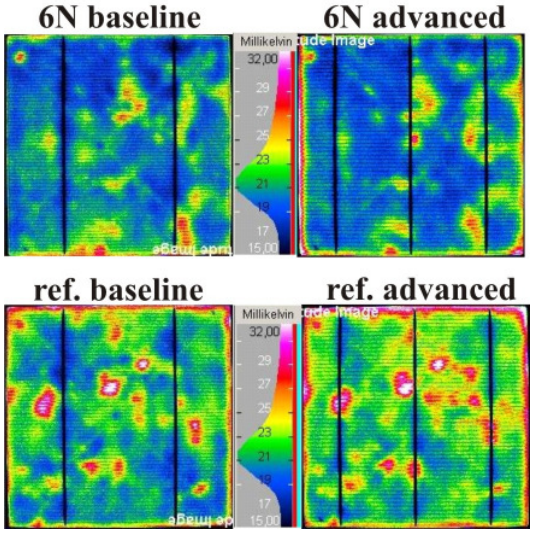

Figure 7: LIT amplitude image of the best baseline and advanced process cells under IR illumination; the 6N cells (top) and the reference cells (bottom) are both pictured in the same colourscale.

Comparing the images it is obvious that the 6N cells show less hotspots than the references from polysilicon. This leads to the conclusion that after the solar cell process remaining contaminants in the 6N material do not lead to significant cell shunting. Comparing the pairs of cells of the same material another observation can be made. Most hotspots are material related and not originate from processing since they are located at the same areas for baseline and advanced process cells.

4.2 Reverse current and breakdown voltage

Reverse characteristics are measured on cells from both, 6N Silicon and reference material. For each material, 2 cells of the bottom, middle and top part are selected. Average current values at -10V are displayed in Figure 7. The reverse characteristic is measured via applying a voltage sweep between 0.2 and -20V to a solar cell in the dark. An example specification of a module manufacturer for the reverse current is that it should be lower than 3 A at -10V.

As shown in Figure 8, all cells reveal a current well below 3A at -10V reverse voltage. What can be observed is that the trend for SoG and reference material is in the opposite direction. As stated by Good et al. [3], the breakdown voltage of a solar cell depends amongst others on the net acceptor density (N_A- N_D). The same is true for the reverse current. The higher (N_A- N_D) gets, the higher will be the reverse current. Since for compensated silicon

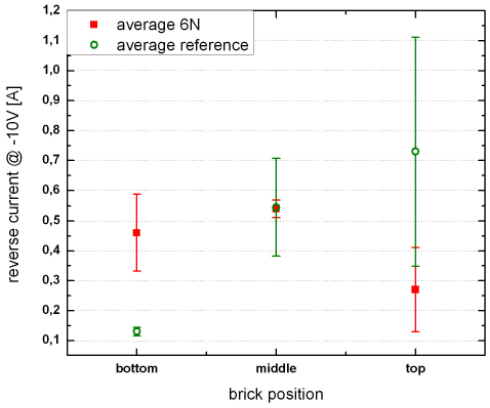

Figure 8: reverse characteristics vs. brick position for 6N and reference cells; the reverse current is measured at -10V.

bricks the net acceptor density decreases from bottom to top, the reverse current decreases with the brick height. The reference from polysilicon shows the opposite, since only acceptors are present in a relevant concentration. That is why here for higher brick positions the reverse current increases as well as the acceptor concentration and resistivity.

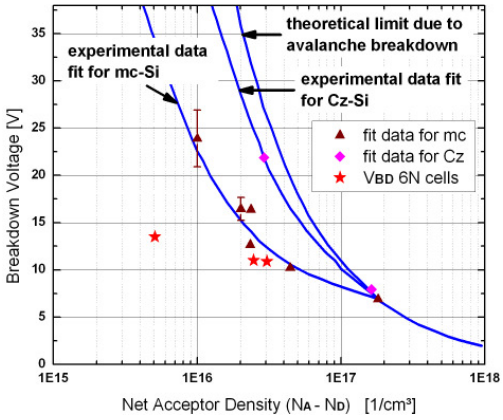

Figure 9: breakdown voltage (V_{BD}) vs. net acceptor density (taken from [3]).

The reverse characteristic also depends on the quality of the surface texture and crystallization [3] which leaves space for further improvements on the process side. Figure 9 shows the dependence of the breakdown voltage of the net acceptor density as published in [3]. In addition, the red stars mark data for the 6N cells. For high net doping (bottom and middle of the brick) the measured values for the 6N cells match with the experimental curve from [3], towards the top of the ingot the influence of surface texture and crystallization govern the breakdown voltage to lower values as expected.

4.3 Light induced degradation

LID on cell level is mainly based on the formation of BO_{2i} complexes and Fe_i under illumination. In our experiment we compare the LID of selected cells of a 6N Silicon and the reference brick. The 6N Silicon brick has a bulk resistivity between 0.6 and 2.7 Ωcm, the reference brick between 1.3 and 0.9 Ωcm. A more detailed study for the same cells can be found in [2]. Figure 10 depicts significant differences of LID depending on the brick position. For both bricks a decrease towards the top of the brick can be observed. This behavior is in good agreement with the assumption that BO_{2i} pairing is a main degradation effect present since the oxygen content decreases towards the top of the ingot. The average relative degradation of the efficiency with 1.4% for 6N Silicon and 1.1% for the reference material are well in standard specification for polysilicon (for a 16% cell ca. 0.2% absolute in efficiency for both materials).

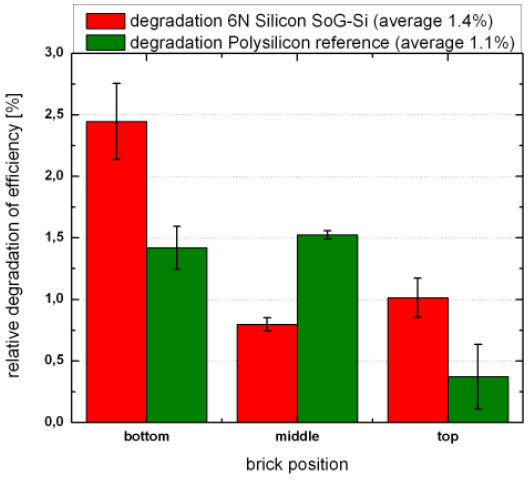

Figure 10: relative degradation of the efficiency for 6N Silicon and reference material for different brick positions.

Both materials show similar LID which is in good agreement with the observations of Kopecek et al. [4] which were confirmed by Mc. Donald et al. [5] that BO_{2i} pairing depends on the net doping only for compensated silicon but not on the total boron content.

5 CONCLUSIONS

We present solar cells made from 100% 6N Silicon solar grade feedstock with average efficiencies of 16% throughout an entire brick. The solar cell process used is a standard industrial type screen printed fire through silicon nitride process. All adaptations which are applied still satisfy industrial standards and are beneficial for the SoG material as well as for the polysilicon reference. Further characterisations show the differences of the cells from SoG-Si compared to the reference cells from polysilicon. IV data reveals a common behaviour for SoG-Si cells also for the 6N material that these cells perform better in V_{OC} and FF but lower in J_{SC}. SR and LBIC reveal a significant gain in emitter response for advanced process cells which still can be improved e.g. by applying e.g. a selective emitter process with a potential efficiency of 17 %. The limitations of the bulk performance for the SoG cells are revealed as well. Operating requirements which are important facts for module assembly are well in the limits of example manufacturers specifications. The reverse current of the cells investigated are well below the current limit of 3A at -10V. The degree of LID is comparable to the one of the polysilicon reference with an average of 0.2% absolute in efficiency.

In conclusion our results show that solar cells made of 6N Silicon SoG feedstock are well suited for industrial production. With minor adaptations to a standard industrial process SoG-Si can be successfully integrated in cell fabrication and as such reduce PV module cost and energy payback time towards the point of grid parity.

ACKNOWLEDGEMENT

Most of this work was done within the New Process project funded by the Norwegian Research Council (NRC) and Umoe Solar AS.

REFERENCES

[1] K. Peter et al., “FUTURE POTENTIAL FOR SOG-SI FEEDSTOCK FROM THE METALLURGICAL PROCESS ROUTE” Proceedings of the 23rd European Photovoltaic Solar Energy Conference, Valencia, Spain WIP Renewable Energies, Munich, Germany, 2008

[2] A. Halm, J. Jourdan, S. Nichol, B. Ryningen, H. Tathgar, R. Kopecek, “LARGE AREA INDUSTRIAL SOLAR CELLS ON LOW COST 100% MC SOG SI SUBSTRATES: EFFICIENCIES EXCEEDING 16%”, Proceedings of the 35th IEEE PVSEC Honolulu, USA, June 2010

[3] E. A. Good, R. Kopecek and J. Arumughan, “Surface Texture and Dopant Density Influences on Junction Breakdown in Compensated Solar Grade Silicon Substrates” Crystal Clear Workshop: Arriving at Well-Founded Solar Grade Silicon Feedstock Specifications, 11.14.2008

[4] R. Kopecek, K. Peter, E. A. Good, J. Libal, M. Acciari, S. Binetti, “CRYSTALLINE Si SOLAR CELLS FROM COMPENSATED MATERIAL: BEHAVIOR OF LIGHT INDUCED DEGRADATION” Proceedings of the 23rd European Photovoltaic Solar Energy Conference, Valencia, Spain WIP Renewable Energies, Munich, Germany, 2008, p. 1218

[5] D. Macdonald, F. Rougieux, A. Cuevas, B. Lim, J. Schmidt, M. Di Sabatino, and L. J. Geerligs, "Light-induced boron-oxygen defect generation in compensated *p*-type Czochralski silicon" J. Appl. Phys. 105, 093703 , 2009